

## Boundary Layer Thickness and Friction Velocity by Symmetry Arguments

Chenning Tong\*

*Department of Mechanical Engineering, Clemson University, Clemson, South Carolina 29631, USA*



(Received 18 February 2023; accepted 22 April 2024; published 16 May 2024)

We derive analytically for the first time the downstream evolution of the boundary layer thickness and the friction velocity of the zero-pressure-gradient turbulent boundary layer (ZPGTBL). Lie groups were used to derive the downstream evolution and to obtain the full set of the similarity variables and the leading-order similarity equations. An approximate leading-order solution was obtained using matched asymptotic expansions. The similarities and differences between ZPGTBL and turbulent channel flows in terms of the similarity equations are discussed to support the notion of leading-order universality of the near-wall layer.

DOI: [10.1103/PhysRevLett.132.204001](https://doi.org/10.1103/PhysRevLett.132.204001)

*Introduction.*—The zero-pressure-gradient turbulent boundary layer (ZPGTBL) is one of the most important flows to understand the physics of turbulence, and has been studied extensively (e.g., [1–12]). Essential to the understanding of a boundary layer is its similarity solution. The zero-pressure-gradient laminar boundary layer (the Blasius boundary layer, [13]) has the well-known similarity solution, a key part of which is the downstream evolution of the boundary layer thickness and the surface stress.

Over the past decades there have been many efforts devoted to finding a similarity solution of ZPGTBL. Tennekes and Lumley [14] derived a leading-order mean momentum similarity equation. Mellor [15] obtained the log law. However, prediction of the boundary layer thickness and the wall shear stress, without which the similarity variables cannot be fully defined, has proven to be much more challenging and has not been made successfully. Tennekes and Lumley [14] used the boundary layer thickness  $\Delta$  defined by [5] using an integral quantity, not derived from the boundary layer parameters, as done for the Blasius boundary layer. Its downstream evolution and the friction velocity were not predicted. A Lie group analysis was performed in [16] to find a linear growth of the boundary layer thickness, which is inconsistent with experimental evidence (e.g., [17]). The same definition of  $\Delta$  as [14] was used in [18], but did not provide an expression for it. The analysis in [19] attempted to obtain a similarity solution using the Reynolds-averaged boundary layer equations without the viscous terms. However, as we show in this work, their equations do not have a valid similarity solution.

In this work we derive analytically for the first time the evolution of the boundary layer thickness,  $\delta$ , whose definition is not predetermined and will come from the analysis, the evolution of the friction velocity, the full set of similarity variables, and the ordinary differential (similarity) equations. We will perform a symmetry analysis of the Reynolds-averaged boundary layer equations and then

employ the method of matched asymptotic expansions to obtain an approximate solution.

Parallel to the research on ZPGTBL, there also has been much effort to investigate turbulent channel and pipe flows, which are amenable to more rigorous asymptotic analysis (e.g., [20,21]). The near-wall (or inner) layers of these flows are widely believed to have much in common, i.e., the near-wall layers are universal. There is also evidence against universality (e.g., [10,17,22]). However, there have been essentially no theoretical analyses on the similarities and differences between these flows. The present work will also help shed some light on the important issue of the universality of the near-wall layers.

*Symmetry analysis.*—One of the symmetries of the Navier-Stokes equations is invariance under a one-parameter Lie dilation group (e.g., [23,24]). A key requirement for this invariance is a fixed Reynolds number. However, it has long been recognized that energy-containing statistics in turbulent flows at high Reynolds numbers are approximately Reynolds number invariant. This approximate invariance is associated with spontaneous breaking of the symmetries of the Navier-Stokes equations from laminar to turbulent flows. Therefore, while the symmetries of laminar flows are exact, the symmetries of turbulent flows are only approximate. The concept of spontaneous symmetry breaking and approximate symmetry first emerged in condensed matter physics and later were key to predicting certain nonzero mass particles in Yang-Mills gauge fields ([25–27]). In the present work, we seek the leading-order symmetries and similarity properties of ZPGTBL. Therefore, Reynolds number invariance of energy-containing statistics is the only physical assumption used.

We use Lie dilation groups to analyze the leading-order symmetries (group transformation properties) of the ZPGTBL equations: the mean momentum equation, the Reynolds stress budget, and the mean continuity equation. The groups will be used to derive the evolution of the

boundary layer thickness and the Reynolds shear stress and to obtain the similarity variables.

To obtain the leading-order symmetries, we recognize that at high Reynolds numbers the outer layer is approximately Reynolds number independent and whereas the inner layer depends on the viscosity. Therefore, we need to derive the leading-order equations for the two layers and analyze their symmetries separately.

*Outer layer symmetry.*—For the outer layer, the leading-order symmetries (or the symmetries of the leading-order equations) need to be obtained with the Reynolds-number-dependent terms dropped. These symmetries are similar in nature to the approximate symmetries previously investigated (e.g., [28]). It is easily shown that by dropping the viscous term in the mean momentum equation, as done by [19], the group leads to a boundary layer thickness  $\delta \propto x$  and  $\overline{uv} = \text{const}$ , inconsistent with the behaviors of ZPGTBL. The reason is that there are other higher-order terms in the equations that do not contain the viscosity, but are implicitly Reynolds-number dependent. They also need to be identified and dropped.

To identify the higher-order terms, we perform an order of magnitude analysis of the equations. We first consider the scaling of the velocity defect  $U - U_e \sim U_e$  proposed in [19], where  $U$  and  $U_e$  are the mean streamwise velocity and the free-stream velocity respectively. With this scaling, the shear production of the turbulent kinetic energy (TKE) would scale as  $-\overline{uv}(\partial U/\partial y) \sim u_*^2 U_e/\delta$ , where  $y$  is the wall-normal direction ( $x$  and  $z$  are the streamwise and spanwise directions, respectively, and  $u$ ,  $v$ , and  $w$  are the corresponding velocity fluctuations, respectively, hereafter). Since

shear production is the only production mechanism, the TKE would scale as  $k \sim U_e^2$ . The dissipation would scale as  $k^{3/2}/\delta \sim U_e^3/\delta$  ([29], based on Reynolds number invariance), asymptotically larger than the production, indicating that the scaling  $U - U_e \sim U_e$  is inconsistent with the scaling of the dissipation. Furthermore, it can be easily seen that only  $U - U_e \sim u_*$  (and  $\partial U/\partial y \sim u_*/\delta$ ) will result in the same scaling for the dissipation and the shear production.

With  $U - U_e \sim u_*$ , we perform an order of magnitude analysis [30] to identify the leading-order terms in the equations, which are Reynolds number invariant. The leading-order mean momentum equation is

$$U_e \partial_x U = -\partial_y \overline{uv}. \quad (1)$$

Similarly, we obtain the leading-order shear stress budget and TKE budget,

$$U_e \partial_x \overline{uv} = -\overline{(u \partial_y p + v \partial_x p)} - \overline{v^2} \partial_y U, \quad (2)$$

$$U_e \partial_x k = -\overline{uv} \partial_y U - \partial_y \overline{p v} - \overline{\partial_y (u^2 + v^2 + w^2)} v/2 - \epsilon. \quad (3)$$

The velocity-pressure gradient term in the shear stress budget scales the same as production. The pressure transport and turbulent transport terms in the TKE budget scale the same as production. Therefore, they should dilate in the same way as the production terms. The finite form of the dilation group is

$$\begin{aligned} \tilde{x} &= e^a x, & \tilde{y} &= e^b y, & \tilde{U} &= U, & \tilde{U} - U_e &= e^g (U - U_e), \\ \partial \tilde{U} &= e^g \partial U, & \tilde{V} &= e^c V, & \tilde{\overline{uv}} &= e^{d_2} \overline{uv}, & \tilde{u^2} &= e^{d_1} u^2, & \tilde{v^2} &= e^{d_1} v^2, \end{aligned} \quad (4)$$

where  $a$ ,  $b$ , etc., are the group parameters. For the equations to be invariant the exponents must satisfy  $g - a = d_2 - b$ ,  $d_2 - a = d_1 + g - b$ , and  $d_1 - a = d_2 + g - b = 3d_1/2 - b$ , respectively, leading to  $d_2 = d_1 = 2b - 2a$  and  $g = b - a$ , and hence a two-parameter dilation group.

To obtain a one-parameter group an additional relationship is needed. In principle, it can be obtained by asymptotically matching the outer and inner layers. Here, we instead use an ansatz, the logarithmic friction law. We will show later that the group does indeed lead to the logarithmic friction law. The friction law dilates as

$$\frac{U_e}{u_* e^g} = \frac{1}{\kappa} \ln \frac{u_* \delta e^{g+b}}{\nu} + D = \frac{1}{\kappa} \left( \ln \frac{u_* \delta}{\nu} + g + b \right) + D. \quad (5)$$

Note that  $\delta$  as a function of  $x$  is not yet known, and therefore is not fully defined. Since (5) is invariant under

the dilation group, we have

$$\frac{U_e}{u_*} = e^g \left\{ \frac{1}{\kappa} \left( \ln \frac{u_* \delta}{\nu} + g + b \right) + D \right\} = \frac{1}{\kappa} \ln \frac{u_* \delta}{\nu} + D. \quad (6)$$

Therefore,

$$(e^g - 1) \left\{ \frac{1}{\kappa} \ln \frac{u_* \delta}{\nu} + D \right\} = (e^g - 1) \frac{U_e}{u_*} = -\frac{g+b}{\kappa} e^g. \quad (7)$$

This equation provides an implicit relationship between  $g$  and  $b$ . Rather than directly solving (7) we examine infinitesimal forms of the group with exponents  $dg$ ,  $da$ ,  $db$ , etc. Taylor expanding the second and third terms in (7) and keeping the leading-order terms we have

$$dg \frac{U_e}{u_*} = -\frac{dg + db}{\kappa} \text{ or } dg = \frac{-db}{\kappa \frac{U_e}{u_*} + 1} = \frac{-da}{\kappa \frac{U_e}{u_*} + 2}. \quad (8)$$

From the continuity equation, we have  $dg - da = dc - db$ ,  $dc = 2dg$ . We obtain a one-parameter group

$$\tilde{x} = e^{da}x, \quad \tilde{y} = e^{db}y, \quad \tilde{U} - U_e = e^{dg}(U - U_e), \quad \tilde{V} = e^{2dg}V, \\ \widetilde{uv} = e^{2dg}\overline{uv}, \quad \widetilde{u^2} = e^{2dg}\overline{u^2}, \quad \widetilde{v^2} = e^{2dg}\overline{v^2}, \quad \widetilde{u_*} = e^{dg}u_*. \quad (9)$$

Note that  $\delta$  dilates in the same way as  $y$ . From (9) we obtain the characteristic equations of the group

$$\frac{du_*}{u_*} = -\frac{dy}{y(\kappa\frac{U_e}{u_*} + 1)} = -\frac{d\delta}{\delta(\kappa\frac{U_e}{u_*} + 1)} = -\frac{dx}{x(\kappa\frac{U_e}{u_*} + 2)} \\ = \frac{d(U - U_e)}{U - U_e} = \frac{dV}{2V}. \quad (10)$$

From the first and fourth terms we obtain (without the dimensional integration constant)  $x \sim u_*^{-2}e^{\kappa U_e/u_*}$ . Its non-dimensional form is

$$U_e x/\nu = \text{Re}_x \sim (U_e^2/u_*^2)e^{\kappa U_e/u_*}. \quad (11)$$

Similarly, we obtain  $\delta \sim u_*^{-1}e^{\kappa U_e/u_*}$ ,  $V \sim u_*^2$ . The non-dimensional form of  $\delta$  is

$$U_e \delta/\nu = \text{Re}_\delta \sim (U_e/u_*)e^{\kappa U_e/u_*}. \quad (12)$$

Equations (11) and (12) are functions of  $U_e/u_*$ , which can be used as a parameter to obtain the dependence of  $\delta$  on  $x$ . These are the central results of the present work and to our best knowledge, are the first analytic derivation of the downstream evolution of the friction velocity and the boundary layer thickness.

The first and last two terms in (10) result in  $U - U_e \sim u_*$  and  $V \sim u_*^2$ . Nondimensionalizing the variables using  $x$ ,  $u_*$ , and  $U_e$ , we obtain for the first time the full set of the similarity variables for the outer layer  $U_o = (U - U_e)/u_*$ ,  $V_o = VU_e/u_*^2$ ,  $y_o = yU_e/(xu_*)$ ,  $\overline{uv}_o = \overline{uv}/u_*^2$ ,  $\overline{u_o^2} = \overline{u^2}/u_*^2$  and  $\overline{v_o^2} = \overline{v^2}/u_*^2$ . Here  $y_o$  is defined using the boundary layer parameters ( $x$ ,  $U_e$ , and  $u_*$ ), in a similar way to the Blasius boundary layer.

*Inner layer symmetry.*—We now perform a Lie group analysis of the leading-order inner equations. The leading-order mean momentum equation is [14]

$$0 = -\partial_y \overline{uv} + \nu \partial_y^2 U. \quad (13)$$

The dilation group is  $\tilde{y} = e^b y$ ,  $\tilde{U} = e^g U$ ,  $\widetilde{\overline{uv}} = e^{2g}\overline{uv}$ . The transformation for  $\overline{uv}$  is identical to the outer layer because it scales with  $u_*^2$  in both layers. For (13) to be invariant, the exponents must satisfy  $2g - b = g - 2b$ ,  $b = -g$ . From the continuity equation, we have  $g - a = c - b$ ,  $c = -a$ . These group parameters are also consistent with the dilation properties of the Reynolds shear stress and TKE budgets. The group now is

$$\tilde{x} = e^a x, \quad \tilde{y} = e^{-g} y, \quad \tilde{U} = e^g U, \quad \tilde{V} = e^{-a} V, \quad \widetilde{\overline{uv}} = e^{2g}\overline{uv}, \quad (14)$$

where  $a$  and  $g$  are related by (7). The characteristic equations for the group are

$$\frac{du_*}{u_*} = -\frac{dy}{y} = -\frac{dx}{x(\kappa\frac{U_e}{u_*} + 2)} = \frac{dV}{V(\kappa\frac{U_e}{u_*} + 2)}. \quad (15)$$

The first two terms result in  $u_* \sim y^{-1}$ . The last two terms lead to  $V \sim x^{-1}$ . We obtain the similarity variables for the inner layer  $U_i = U/u_*$ ,  $V_i = Vx/\nu$ ,  $y_i = yu_*/\nu = y^+$ ,  $\overline{uv}_i = \overline{uv}/u_*^2$ ,  $\overline{u_i^2} = \overline{u^2}u_*^2$ ,  $\overline{v_i^2} = \overline{v^2}u_*^2$ , where  $V_i$  has not been properly defined previously in the literature.

*Approximate solution using matched asymptotic expansions.*—In a typical Lie group analysis, after the symmetries are identified and the similarity variables are obtained, the similarity equations are derived and their solution is sought. In the case of turbulent flows, the similarity equations are unclosed and cannot be solved without a turbulence model. However, matching the outer and inner asymptotic expansions effectively closes the equations, allowing us to obtain an approximate solution without a turbulence model.

We write the outer layer similarity variables as asymptotic expansions

$$U_o(y_o, \text{Re}_*) = U_{o1}(y_o) + \text{higher-order terms}, \\ \overline{uv}_o(y_o, \text{Re}_*) = \overline{uv}_{o1}(y_o) + \text{higher-order terms}, \quad (16)$$

where the similarity variables,  $U_{o1}$ , etc. are of order 1. Substituting (16) into the mean momentum equation, we obtain the leading-order similarity equation for  $U_o$

$$-y_o d_{y_o} U_{o1} = -d_{y_o} \overline{uv}_{o1}, \quad (17)$$

which is identical to that obtained by [14]. However, their definition of  $y_o$  is different. Similarly, the leading-order shear-stress budget is

$$-y_o d_{y_o} \overline{uv}_{o1} = -(\overline{u\partial_y p + v\partial_x p})_o - \overline{v_o^2} d_{y_o} U_{o1}. \quad (18)$$

Since the outer expansions are not valid in the viscous region (the inner layer), inner expansions are also needed.

The inner similarity variables depend on  $y^+$  and  $\text{Re}_*$ . We write them as asymptotic expansions,

$$U_i(y^+, \text{Re}_*) = U_{i1}(y^+) + \text{higher-order terms}, \\ \overline{uv}_i(y^+, \text{Re}_*) = \overline{uv}_{i1}(y^+) + \text{higher-order terms}. \quad (19)$$

We obtain the leading-order inner similarity equations

$$0 = -d_{y^+} \overline{uv} + d_{y^+}^2 U_i, \quad (20)$$

$$0 = -(\overline{u \partial_y p} + \overline{v \partial_x p})_i - \overline{v_i^2} d_{y^+} U_{i1} + d_{y^+}^2 \overline{uv}_{i1}. \quad (20)$$

We now asymptotically match the outer and inner expansions

$$U = U_e + u_* U_o = U_e + u_* U_{o1}(y_o) + \dots,$$

$$U = u_* U_i = u_* U_{i1}(y^+) + \dots, \quad (21)$$

for  $y_o \ll 1$  and  $y^+ \gg 1$ , resulting the log law (see, e.g., [31] for details)

$$U_{o11} = \frac{1}{\kappa} \ln y_o + C, \quad U_{i11} = \frac{1}{\kappa} \ln y^+ + B, \quad (22)$$

where  $U_{o11}$  and  $U_{i11}$  are the leading-order expansions of  $U_{o1}$  and  $U_{i1}$ , respectively. Inserting (22) into (21) we obtain the dimensional outer and inner expansion as

$$U = U_e + u_* \left\{ \frac{1}{\kappa} \ln y_o + C + \dots \right\}, \quad U = u_* \left\{ \frac{1}{\kappa} \ln y^+ + B + \dots \right\}. \quad (23)$$

From (23) we obtain the logarithmic friction law

$$\frac{U_e}{u_*} = \frac{1}{\kappa} \ln \frac{y^+}{y_o} + B - C = \frac{1}{\kappa} \ln \frac{u_*^2 x}{U_e \nu} + B - C. \quad (24)$$

Using (11)–(12) we have  $\delta \sim x u_* / U_e$ . The friction law can then be written as (5), confirming the ansatz used above to obtain the outer layer symmetry is indeed part of the unique solution of the leading-order equations. Similarly, we obtain the matching results for the leading-order Reynolds shear stress as  $\overline{uv} = u_*^2 (-1 + y_o / \kappa)$ . One can also write down the expansions for the velocity-pressure-gradient terms and obtain matching results (not done here). With (11)–(12) and the fully defined similarity variables, (22) and  $\overline{uv} = u_*^2 (-1 + y_o / \kappa)$  satisfy (1) to the leading order, verifying them [and (5) and (24)] as part of the unique similarity solution of the ZPGTBL equations. The solution also provide the downstream variations of the mean velocity and shear stress profiles, which previously were not available.

We now make preliminary comparisons of the theoretical prediction (11) and (12) of the nondimensional velocity  $U_e / u_*$  (equivalent to the surface shear stress) and the nondimensional outer layer thickness  $\text{Re}_\delta = U_e \delta_{99} / \nu$  (both as functions of the nondimensional downstream distance  $\text{Re}_x = U_e x / \nu$ ) with the experimental data of [17] (the SP40 configuration). The measured values of  $U_e / u_*$  are used as the parameter to obtain the theoretical values of  $\text{Re}_x$  and  $\text{Re}_\delta$ . The theoretical prediction contains several nondimensional coefficients that need to be obtained using experimental data: The von Kármán constant  $\kappa = 0.420$  and the

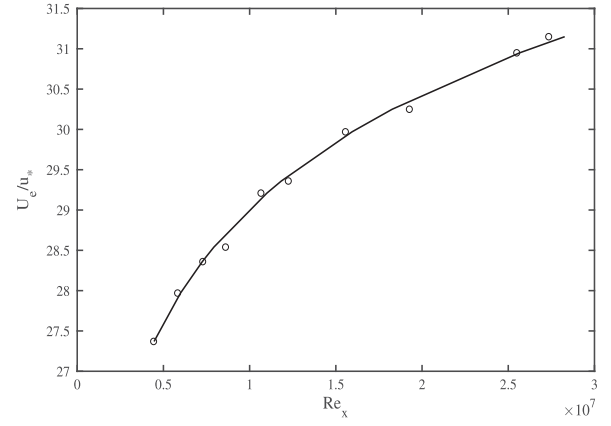


FIG. 1.  $U_e / u_*$  vs the nondimensional downstream distance  $\text{Re}_x = U_e x / \nu$ . Circles: experimental data from Marusic [17] (the SP40 configuration); solid line: theoretical prediction of Eq. (25).

nondimensional coefficient for  $\delta_{99}$  are obtained by fitting (12) to the experimental data; The virtual origin of  $x = -1.744$  m and the nondimensional coefficient for  $\text{Re}_x$  are then obtained by fitting (11) to the data. In particular, the values of  $U_e / u_*$  and  $\delta_{99}$  at  $x = 1.6$  m are used to determine the nondimensional coefficients. The kinematic viscosity is taken as the value in [17],  $\nu = 15.1 \times 10^{-6}$  m<sup>2</sup>/s. The results are

$$\text{Re}_x = 0.06024 \frac{U_e^2}{u_*^2} e^{\kappa U_e / u_*}, \quad \text{Re}_\delta = 0.02204 \frac{U_e}{u_*} e^{\kappa U_e / u_*}. \quad (25)$$

We then have  $\delta_{99} = 0.3659 x u_* / U_e$ ,  $y_o = 0.3659 y / \delta_{99}$ .

Figures 1 and 2 show that with these coefficients, the analytic prediction, especially the functional forms, has an excellent agreement with the experiments. However,  $\kappa = 0.420$  obtained here based on the boundary layer thickness and the friction velocity, which are global behaviors, is quite different from 0.384 obtained in the same experiment and by [10] using the mean velocity profile, a local

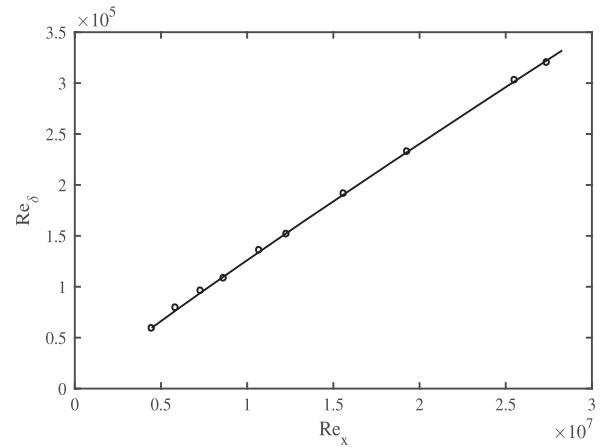


FIG. 2. Nondimensional boundary layer thickness  $\text{Re}_\delta = U_e \delta / \nu$  vs  $\text{Re}_x$ . Legend: same as in Fig. 1.

behavior, but is much closer to that of [32] (0.40) and the typical value of 0.421 in pipe flows ([22,33]). We emphasize that these are preliminary comparisons with a single experiment. It is therefore unclear whether the different values are a coincidence or an indication of the differences in the two ways of estimating the von Kármán. This issue requires further attention in future studies.

*Universality of near-wall layer.*—The leading-order equations allow us to compare ZPGTBL with channel flows to examine the key question of near-wall universality. In the inner layer the mean momentum equation is dominated by the Reynolds stress and viscous stress terms [ [21] and Eq. (20)] in both flows. The Reynolds shear stress budgets also have similar properties in both flows, being dominated by the production, pressure, and viscous terms [ [34] and Eq. (20)] (the similarity variables are also defined in the same way), indicating that the two flows have the same leading-order structure.

This issue can be further examined using the outer equations. In channel flows, the Reynolds shear stress budget is a balance between shear production and velocity-gradient–pressure interaction ([34]). The mean velocity gradient is “adjusted” to balance the Reynolds stress budget. The leading-order mean momentum equation is a balance between the shear stress derivative and the mean pressure gradient ([21]), with the latter imposing the linear variation of the leading-order (linear) variation of the Reynolds shear stress.

In ZPGTBL the Reynolds shear stress balance [Eq. (18)] is among the mean advection, production, and velocity gradient–pressure interaction. However, in the log layer ( $y_o \ll 1$ ), the advection term is of higher order. Therefore the balance in the log layer is asymptotically identical to that in channel flows. While the mean momentum balance (17) is between the mean advection and the shear stress derivative, the log law ensures the leading-order (linear) variation of the Reynolds shear stress. Therefore, from the perspective of both the inner and outer equations, the leading-order near-wall structure of channel flows and ZPGTBL are the identical, supporting the notion of universality of the leading-order near-wall turbulence. The differences observed in experiments are potentially due to higher-order effects, which deserve further attention.

*Conclusions.*—We performed a symmetry analysis of the equations for ZPGTBL using Lie dilation groups, and obtained local, leading-order symmetries of the equations. We derived for the first time the evolution of the boundary layer thickness and the shear stress, and the full set of similarity variables. Using the asymptotic expansions the leading-order similarity equations for the outer and inner layers were obtained. Matching the expansions resulted in an approximate similarity solution in the overlapping layer, the log law. The leading-order equations for both the channel flows and ZPGTBL show similar

properties in the near wall layer, supporting the notion of its universality.

The author thanks Professor Katepalli Sreenivasan for encouraging him to look into issues in classical engineering turbulent boundary layers and for providing valuable comments on the manuscript. This work was supported by the National Science Foundation under Grant No. AGS-2054983.

---

\*ctong@clemson.edu

- [1] L. Prandtl, Bericht über die Entstehung der Turbulenz, *Z. Angew. Math. Mech.* **5**, 136 (1925).
- [2] T. von Kármán, Mechanische Ähnlichkeit und Turbulenz, in *Proceedings of the Third International Congress Applied Mechanics*, Stockholm (1930), pp. 85–105.
- [3] P. S. Klebanoff, Characteristics of turbulence in a turbulent boundary layer with zero pressure gradient, Technical Note, TN3178 NACA (1954).
- [4] H. Schlichting, *Boundary Layer Theory* (McGraw Hill Book Company, New York, New York, 1956).
- [5] F. H. Clauser, The turbulent boundary layer, *Adv. Appl. Mech.* **56**, 4 (1956).
- [6] A. S. Monin and A. M. Yaglom, *Statistical Fluid Mechanics* (MIT Press, Cambridge, MA, 1971).
- [7] K. R. Sreenivasan, The turbulent boundary layer, in *Lecture Notes in Physics* (Springer, New York, 1989), pp. 159–209.
- [8] S. B. Pope, *Turbulent Flows* (Cambridge University Press, Cambridge, England, 2000).
- [9] B. J. McKeon and Sreenivasan, Introduction: Scaling and structure in high Reynolds number wall-bounded flows, *Phil. Trans. R. Soc. A* **365**, 635 (2007).
- [10] H. M. Nagib, K. A. Chauhan, and P. A. Monkewitz, Approach to an asymptotic state for zero pressure gradient turbulent boundary layers, *Phil. Trans. R. Soc. A* **365**, 755 (2007).
- [11] I. Marusic, B. J. McKeon, P. A. Monkewitz, H. M. Nagib, and A. J. Smits, Wall-bounded turbulent flows at high Reynolds numbers: Recent advances and key issues, *Phys. Fluids* **22**, 065103 (2010).
- [12] A. J. Smits, B. J. McKeon, and I. Marusic, High-Reynolds number wall turbulence, *Annu. Rev. Fluid Mech.* **43**, 353 (2011).
- [13] H. Blasius, Grenschichten in flüssigkeiten mit kleiner reibung, *Z. Math. Phys.* **56**, 1 (1908).
- [14] H. Tennekes and J. L. Lumley, *A First Course in Turbulence* (MIT Press, Cambridge, MA, 1972).
- [15] G. Mellor, The large Reynolds number, asymptotic theory of turbulent boundary layers, *Int. J. Eng. Sci.* **10**, 851 (1972).
- [16] M. Oberlack and G. Khujadze, Symmetry methods in turbulent boundary layer theory: New wake region scaling laws and boundary layer growth, in *IUTAM Symposium on One Hundred Years of Boundary Layer Research*, edited by G. Meier, K. Sreenivasan, and H.-J. Heinemann (Springer, New York, 2006), pp. 39–48.
- [17] I. Marusic, K. A. Chauhan, V. Kulandaivelu, and N. Hutchins, Evolution of zero-pressure-gradient boundary

- layers from different tripping conditions, *Fluid Mech.* **783**, 379 (2015).
- [18] P. A. Monkewitz, K. A. Chauhan, and H. M. Nagib, Self-contained high Reynolds-number asymptotics for zero-pressure-gradient turbulent boundary layers, *Phys. Fluids* **19**, 115101 (2007).
- [19] W. K. George and L. Castillo, Zero pressure gradient turbulent boundary layer, *Appl. Mech. Rev.* **50**, 689 (1997).
- [20] C. B. Millikan, A critical discussion of turbulent flows in channels and circular tubes, *Proceedings of the Fifth International Conference Applied Mechanics*, Cambridge, MA (1938).
- [21] N. Afzal, Millikan's argument at moderately large Reynolds number, *Phys. Fluids* **19**, 600 (1976).
- [22] B. J. McKeon and J. F. Morrison, Asymptotic scaling in turbulent pipe flow, *Phil. Trans. R. Soc. A* **365**, 771 (2007).
- [23] G. W. Bluman and S. Kumei, *Symmetry and Differential Equations* (Springer, New York, USA, 1989).
- [24] B. J. Cantwell, *Introduction to Symmetry Analysis* (Cambridge University Press, Cambridge, England, 2002).
- [25] P. W. Higgs, Broken symmetries and the masses of gauge bosons, *Phys. Rev. Lett.* **13**, 508 (1964).
- [26] P. W. Higgs, Nobel lecture: Evading the Goldstone theorem, *Rev. Mod. Phys.* **86**, 851 (2014).
- [27] E. Castellani, On the meaning of symmetry breaking, in *Symmetries in Physics: Philosophical Reflections* (Cambridge University Press, Cambridge, England, 2003), pp. 1–17.
- [28] V. N. Grebenev and M. Oberlack, Approximate symmetries of the Navier-Stokes equations, *J. Nonlinear Math. Phys.* **14**, 157 (2007).
- [29] G. I. Taylor, Statistical theory of turbulence. i-iv, *Phil. Trans. R. Soc. A* **151**, 421 (1935).
- [30] See Supplemental Material at <http://link.aps.org/supplemental/10.1103/PhysRevLett.132.204001> for the order of magnitude analysis of the boundary layer equations in the outer layer.
- [31] C. Tong and M. Ding, Velocity-defect laws, log law and logarithmic friction law in the convective atmospheric boundary layer, *J. Fluid Mech.* **883**, A36 (2020).
- [32] M. Vallikivi, H. M., and A. J. Smits, Turbulent boundary layers statistics at very high Reynolds number, *J. Fluid Mech.* **779**, 371 (2015).
- [33] B. J. McKeon, J. Li, W. Jiang, J. F. Morrison, and A. J. Smits, Further observations on the mean velocity distribution in fully developed pipe flow, *Fluid Mech.* **501**, 135 (2004).
- [34] S. Hoyas and J. Jimenes, Reynolds number effects on the Reynolds-stress budgets in turbulent channels, *Phys. Fluids* **20**, 101511 (2008).